THE JOURNAL OF BIOLOGICAL CHEMISTRY VOL. 281, NO. 41, pp. 30621–30630, October 13, 2006

Identification of Novel Glycogen Synthase Kinase-3β Substrate-interacting Residues Suggests a Common Mechanism for Substrate Recognition*

Received for publication, May 15, 2006, and in revised form, August 7, 2006 Published, JBC Papers in Press, August 7, 2006, DOI 10.1074/jbc.M604633200

Ronit Ilouz[‡1], **Noga Kowalsman**[§2], **Miriam Eisenstein**[¶2], **and Hagit Eldar-Finkelman**[‡3]

From the [‡]*Department of Human Molecular Genetics and Biochemistry, Sackler School of Medicine, Tel-Aviv University, Tel Aviv 69978, Israel and the Departments of* [§]*Biological Chemistry and* [¶]*Chemical Research Support, Weizmann Institute of Science, Rehovot 76100, Israel*

Substrate recognition and specificity are essential for the reliability and fidelity of protein kinase function. GSK-3 has a unique substrate specificity that requires prior phosphorylation of its substrates. However, how the enzyme selects its phosphorylated substrates is unknown. Here, we combined *in silico* modeling with mutagenesis and biological studies to identify GSK-3-substrate interaction sites located within its binding cleft. Protein-protein docking of GSK-3β and the phosphorylated cAMP responsive element binding protein (pCREB) (using the available experimentally determined structures), identified Phe[67], Gln[89], and Asn[95] of GSK-3β as putative binding sites interacting with the CREB phosphorylation motif. Mutations of these residues to alanine impaired GSK-3β phosphorylation of several substrates, without abrogating its autocatalytic activity. Subsequently, expression of the GSK-3β mutants in cells resulted in decreased phosphorylation of substrates CREB, IRS-1, and β-catenin, and prevented their suppression of glycogen synthase activity as compared with cells expressing the wild-type GSK-3β. Our studies provide important additional understanding of how GSK-3β recognizes its substrates: In addition to prior phosphorylation typically required in GSK-3 substrates, substrate recognition involves interactions with GSK-3β residues: Phe[67], Gln[89], and Asn[95], which confer a common basis for substrate binding and selectivity, yet allow for substrate diversity.

Glycogen synthase kinase 3 (GSK-3)[4] is a ubiquitous serine/threonine kinase expressed as two isoforms (α and β) (1), and has been implicated in many biological processes, including glucose metabolism, cell apoptosis, and embryonic development (reviewed in Refs. 2–4). The cellular activity of GSK-3 is stringently controlled in response to growth factors and hormones. However, unlike most protein kinases, GSK-3 is constitutively active in resting cells and becomes inhibited upon stimulation of the cells. This inhibition is achieved through direct phosphorylation of N-terminal serine residues (Ser^{21} or Ser^{9} in α, β, respectively) by several protein kinases, such as PKB, p90RSK, PKA, and PKC (2–4). GSK-3 also may be phosphorylated on Tyr^{216} located in the activation loop (5). This phosphorylation is an autophosphorylation event as demonstrated by *in vitro* and *in vivo* cell systems (5–7).

Elevated activity of GSK-3 is associated with several diseases, including type 2 diabetes, neurodegenerative diseases, and affective disorders (8–10). Hence, selective inhibitors of GSK-3 may be of therapeutic value and are currently under extensive development (11–14). Thus, understanding of how GSK-3 interacts with its substrates may pave the way for design and development of new specific substrate competitive GSK-3 inhibitors.

Substrate specificity of protein kinases is a fundamental determinant for the integrity and fidelity of signaling pathways. Previous studies formulated consensus sequences for optimal phosphorylation motifs of protein kinases using oriented peptide libraries, bioinformatics, and computational molecular modeling (15–19). The increasing number of three-dimensional structures of protein kinases complexed with substrates had provided an important basis for understanding the mechanism of molecular recognition (20–23). Still, our knowledge of the mechanisms by which protein kinases recognize their substrates is rather limited. GSK-3 has a unique substrate specificity that requires prior phosphorylation of its substrates in the context motif S*XXX*S(p), where S(p) is the phosphorylated "priming" site (24–26).

The three-dimensional structure of GSK-3β showed that three basic residues within the catalytic core, Arg^{96}, Arg^{180}, and Lys^{205}, form a positive pocket that most likely serves as the docking site for the phosphorylated moiety of GSK-3 substrates (27–29). GSK-3β-binding of Axin and APC was localized to a hydrophobic site in the C-terminal helical domain (29, 30). This interaction site, however, is downstream from the catalytic-substrate binding cleft and is not directly involved in the phosphorylation process (29). Therefore, detailed knowledge of the interactions between the substrate amino acids near the priming phosphorylation site and GSK-3β is still desirable.

* The costs of publication of this article were defrayed in part by the payment of page charges. This article must therefore be hereby marked "*advertisement*" in accordance with 18 U.S.C. Section 1734 solely to indicate this fact.

[1] This author performed this work in partial fulfillment of requirements for a Ph.D. from Sackler School of Medicine.

[2] Supported by a grant from the Kimmelman Center for Macromolecular Structure and Assembly.

[3] To whom correspondence should be addressed: Dept. of Human Molecular Genetics and Biochemistry Sackler School of Medicine, Tel Aviv University, Tel Aviv, 69978, Israel. Tel.: 972-3-640-5307; E-mail: heldar@post.tau.ac.il.

[4] The abbreviations used are: GSK-3, glycogen synthase kinase-3; PKB, protein kinase B; p90RSK, S6 ribosomal protein kinase; PKA, cAMP-dependent protein kinase; PKC, protein kinase C; CREB, cAMP response element-binding protein; CBP, CREB-binding protein; EGFP, enhanced green fluorescence protein; IRS-1, insulin receptor substrate-1; PDB, Protein Data Bank; WT, wild type; UDPG, uridine 5-diphosphate [^{14}C]glucose.

In this study, we sought to determine the important substrate recognition sites in GSK-3β by combining *in silico* protein-protein docking of GSK-3β and the phosphorylated cAMP responsive element-binding protein (pCREB), based on the crystal structures of GSK-3β (28, 31) and the NMR structure of pCREB (32), with biological tools. We present a model structure of the ternary complex of GSK-3β, ATP, and the pCREB peptide. The docking model identified specific electrostatic and hydrophobic interactions between pCREB and three amino acids in GSK-3β. Mutagenesis of these sites impaired GSK-3 ability to phosphorylate CREB, confirming their importance for substrate recognition. Importantly, additional GSK-3 substrates were affected by the mutations as well. Hence, our studies identified novel GSK-3β sites involved in recognition of diverse substrates, and provide important data for rational drug design of compounds targeting GSK-3.

EXPERIMENTAL PROCEDURES

Peptides and Materials—Peptides were synthesized by Genemed Synthesis Inc (San Francisco, USA). p9CREB, ILSRRP-S(p)YR, pIRS-1 RREGGMSRPAS(p)VDG, PGS-1 YRRAAVPP-SPSLSRHSSPSQS(p)EDEEE (where S(p) is a phosphoserine). The following antibodies were used in the study: anti GSK-3β (Transduction laboratory, Lexington, KY), anti-phospho-GSK-3 (Tyr^{216}) and anti-phospho-CREB (Ser^{133}) antibodies were obtained from Upstate Biotechnology (Lake Placid, NY), anti-phospho-CREB ($Ser^{129/133}$) was obtained from BioSource International, Inc (Camarillo, CA), CREB antibody, anti-phospho-β-catenin, or β-catenin antibody were obtained from Cell Signaling Technology (Beverly, MA) and anti-phospho-IRS-1 (Ser^{332}) were described before (33). Radioactive materials were purchased from Amersham Biosciences.

Molecular Modeling—The available x-ray structures of GSK-3β (28, 31), one with phosphorylated Tyr^{216} (PDB (Ref. 34) code 1o9u) and another with bound non-hydrolysable analog of ATP, ANP, (PDB code, 1pyx), were used to model the structure of a phosphorylated GSK-3·ATP complex (using the homology module of InsightII, Accelrys, San-Diego, CA). A model of the ternary complex GSK-3·ATP·CREB was obtained by protein-protein docking, using the program MolFit. The p9CREB fragments (residues 127–135) from the 17 NMR models of pCREB in complex with the co-activator CBP (32) (PDB code, 1kdx) present some backbone variation in the turn region. We selected 3 variants of the p9CREB fragment, with different backbone and side chain conformations. In the first protein-protein docking step, we docked each fragment to the GSK-3·ATP model structure, employing the geometric (35), weighted-geometric (36), geometric-electrostatic (37), and geometric-hydrophobic (38) options in MolFit. Standard translation and rotation grid intervals were used (1.05 Å and 12°, respectively). The surface grid points that belong to the side chains of residues Arg^{96}, Arg^{180}, and Lys^{205} of GSK-3 (the primed phosphate binding site) were up-weighted in the weighted geometric docking search, thereby biasing the docking results to include more models in which these residues interact with any residue of p9CREB. The lists of solutions from the four individual docking scans were intersected. Thus, the final list of models included only models that appeared in all 4 docking searches, and each model was evaluated by a weighted-geometric-electrostatic-hydrophobic complementarity score, which is the sum of the (weighted-geometric) + (geometric-electrostatic − geometric) + (geometric-hydrophobic − geometric) scores.

The first docking step clearly preferred one of the 3 conformers of p9CREB (see "Results" and "Discussion"). In a second docking step, the preferred conformer was extended by including also the N-terminal helix (N-pCREB; residues 119–135) and docked to GSK-3β·ATP. The best GSK-3β·ATP·N-pCREB model, which was very similar to the preferred GSK-3β·ATP·p9CREB model, was refined by testing small local relative rotations of the molecules (±2°, ±4°, and ±6°) and searching for the best shape and chemical complementarity. Next, we superposed each of the 17 NMR structures of pCREB onto the refined GSK-3β·ATP·N-pCREB model, using the common Cα atoms. This showed that although there is a large variation in the positions of the C-terminal helices of pCREB, only a few of them interact with GSK-3β. We selected a model with only few clashes with GSK-3β for the final modeling step, which consisted of 20 iterations of intermittent energy minimizations of the GSK-3β·ATP·pCREB ternary complex and dynamics simulations (10,000 steps of 1fs in each iteration). These computations also included a layer of water molecules around the complex (10-Å thick). We used the Discover-3 module in the InsightII package (Accelrys Inc., San Diego, CA) for these simulations, employing the CVFF force field.

Plasmids and Mutants—We previously described His-tagged GSK-3β construct and GSK-3β in pCMV4 plasmid (6). GSK-3β fused to an N-terminal FLAG-tag was initially cloned into pCMV-Tag 2B (Stratagene) in ECoRV and BamHI1. These 3 expression vectors were used as templates for mutagenesis of GSK-3 by the QuikChange site-directed mutagenesis kit (Stratagene) to replace Phe^{67}, Gln^{89}, Asn^{95}, Glu^{97}, and Ser^{66} to alanine. All constructs were sequenced to confirm the presence of mutations. The sequences of mutagenic oligonucleotides are available from the authors upon request. pCREB-EGFP plasmid was purchased from BD Biosciences Clontech (Palo Alto, CA). pCMV4IRS-1 plasmid was described (33). GFP-β-catenin was kindly provided by Dr. Rina Abersfeld from Tel Aviv University.

Protein Expression in Bacteria—GSK-3β was expressed as His-tagged proteins in BL21(DE3) (Novagen, Darmstadt, Germany), induced by 0.4 mM isopropyl 1-thio-β-D-galactopyranoside overnight at 16 °C. Cells were homogenized with a sonication buffer (50 mM NaH_2PO_4 at pH 8.0, 5% glycerol, 0.25% Tween 20, 0.01% β-mercaptoethanol, 0.1 mM *o*-vanadate, 500 mM NaCl, 25 μg/ml leupeptin, 25 μg/ml aprotinin, 1 μg/ml pepstatin). GSK-3 proteins were purified using TALON metal affinity resin according to the manufacturer's instructions (BD Biosciences Clontech).

Cell Transfections and Protein Purification—HEK-293 cells were grown in Dulbecco's Modified Eagle's Medium, containing 25 mM glucose, 10% fetal calf serum, 2 mM glutamine, 100 units/ml penicillin, and 100 μg/ml streptomycin. HEK-293 cells were transiently transfected with indicated constructs (5 μg each), using calcium phosphate method as described (6). Co-expression used 5 μg each, and expression of GSK-3β mutant proteins was verified by Western blot analysis, using GSK-3β antibody. Cells were lysed in ice-cold buffer G (20 mM

Tris-HCl, pH 7.5, 10 mM β-glycerophosphate, 10% glycerol, 1 mM EGTA, 1 mM EDTA, 50 mM NaF, 5 mM $NaPP_i$, 0.5 mM orthovanadate, 1 mM benzamidine, 10 μg/ml leupeptin, 5 μg/ml aprotinin, 1 μg/ml pepstatin, 500 nM microcystine LR, and 0.5% Triton X-100). Cell extracts were centrifuged for 20 min at 15,000 × *g*. Supernatants were collected, and equal amounts of proteins (20 μg) were boiled with SDS sample buffer and subjected to gel electrophoresis (7.5–12% polyacrylamide gel), transferred to nitrocellulose membranes, and immunoblotted with indicated antibodies. For partial purification, cells were lysed with buffer H (50 mM Tris-HCl, pH 7.3, 1 mM EGTA, 1 mM EDTA, 1 mM orthovanadate, leupeptin, aprotinin, and pepstatin A 25 μg/ml each, 500 nM microcystine LR, and 0.25% Triton X-100) and centrifuged at 15,000 × *g*. The resulting supernatants were passed through DE-52 (Whatman) mini-columns that were equilibrated with buffer H. Flow-through and one wash with buffer H containing 0.02 M NaCl were collected. The amount of each mutant was determined by Western blot analysis of DE-52 preparations with αGSK-3β antibody.

In Vitro Kinase Assays—The GSK-3β mutant proteins purified from bacteria or prepared from HEK-293 cells were incubated with indicated substrates (200 μM) in a reaction mixture (50 mM Tris-HCl, pH 7.3, 10 mM Mg-Acetate, and 0.01% β-mercaptoethanol) together with [γ-^{32}P]ATP (100 μM, 0.5 μCi/assay) for 20 min or as indicated in figure legends. Reactions were stopped, spotted on p81 paper (Whatman) washed with phosphoric acid, and counted for radioactivity, as described (6). For CREB phosphorylation, CREB-EGFP was immunoprecipitated with anti-GFP antibody MBL (Woburn, MA) in complex with protein A-Sepharose. GSK-3 proteins were added to the immunoprecipitates under conditions similar to those described above. In "hot" assays, the reactions were boiled with SDS sample buffer and subjected to gel electrophoresis. In cold assays, the reactions were boiled with SDS sample buffer and subjected to immunoblot analysis with αpCREB$^{129/133}$. Similar experiments were performed in autophosphorylation assays except that the substrate was omitted, and ATP concentration was raised to 300 μM.

Glycogen Synthase Activity—HEK-293 cells expressing GSK-3 mutants transiently were incubated with Dulbecco's modified Eagle's medium-low glucose containing 0.5% bovine serum albumin for 4 h. Cells were scraped into GS buffer (50 mM Tris-HCl, pH 7.8, 100 mM NaF, 10 mM EDTA, 5% glycerol, and protease inhibitors: 20 μg/ml leupeptin, 10 μg/ml aprotinin, 10 mg/ml pepstatin A, 1 mM benzamidine) and centrifuged at 8000 × *g*. Lysates were snap frozen in liquid nitrogen and stored at −80 °C. Glycogen synthase activity was assayed in the supernatants, according to the method of Thomas *et al.* (39) and based on the incorporation of uridine 5-diphosphate [^{14}C]glucose (UDPG) into glycogen. Aliquots of tissue homogenate (15 μl) were incubated with 15 μl of reaction mixture (66.6 mM Tris-HCl, pH 7.8, 32.5 mM KF, 0.8 μCi/μl [^{14}C]UDPG (400 μM), 13 mg/ml glycogen rabbit liver, Sigma) for 20 min at 30 °C, as described (6). The reactions were then spotted on ET31 (Whatman) papers, washed with 66% ice-cold ethanol, and counted for radioactivity. Glycogen synthase assays were measured in the presence of 0.1 mM or 10 mM glucose-6-phosphate (G6P), and their ratio was calculated.

RESULTS AND DISCUSSION

CREB is a GSK-3 substrate phosphorylated directly at Ser^{129} by GSK-3 (40). Similar to other GSK-3 substrates, CREB requires pre-phosphorylation at Ser^{133}, which is carried out by cAMP-dependent kinase (40). A minimal peptide sequence encompassing the CREB phosphorylation motif, termed p9CREB (ILSRRPS(p)YR), was shown in *in vitro* kinase assays to be a GSK-3 substrate (Fig. 1*A*). In addition, these experiments emphasized the importance of phosphorylation. Namely, replacement of phosphorylated serine by serine (CREB) glutamic acid (E9CREB, mimicking phosphorylation) or phosphorylated tyrosine (pY9CREB) practically abolished GSK-3 phosphorylation (Fig. 1*A*).

In Silico Molecular Modeling of the Ternary Complex GSK-3·ATP·pCREB—The structure of the ternary complex GSK-3β·ATP·CREB was modeled as described under "Experimental Procedures." We used the structures of the non-ATP-bound GSK-3β (28) and the ANP-bound GSK-3β (31) to model the complex between phosphorylated GSK-3β and ATP. The two structures differ only slightly in the position of the P-loop, but not in the substrate binding cavity. Hence, the phosphorylated GSK-3β·ATP model was constructed by combining these two structures; the conformation of the P-loop backbone and side chains was as in the ANP-bound GSK-3β, and the conformation of Tyr^{216}(p) was as in the phosphorylated GSK-3β.

Currently, there is only one available structure of pCREB (32) bound to the KIX domain of CBP. pCREB consists of two helices (N- and C-terminal) joined by a loop, and the 17 NMR models of pCREB present considerable variability in the relative position of the N- and C-terminal helices. Our protein-protein docking program MolFit treats the docked molecules as rigid bodies and cannot cope with such structural flexibility. Therefore, we docked pCREB to GSK-3β in steps. First, we docked three representing conformers of p9CREB (residues 127–135) to GSK-3·ATP employing a weighting scheme that emphasized contacts involving the primed binding site of GSK-3β, but did not specify the binding partner (see "Experimental Procedures"). Thus, it was rewarding to find that the first docking step clearly preferred one of the three conformers of p9CREB, and ranked near the top a model in which the primed binding site was occupied by CREB-Ser^{133}(p) (rank 31 out of 9,415 models obtained after intersection; see "Experimental Procedures"). The same model was obtained in the second docking step in which a larger fragment of pCREB (N-pCREB; see "Experimental Procedures") was docked to GSK-3·ATP.

In the GSK-3β·ATP·pCREB model the substrate phosphorylation site, CREB-Ser^{129}, was found at a distance of 5 Å from the γ-phosphate of ATP, adequate for phosphorylation. This was a plausible starting structure for the third modeling step, which consisted of energy minimization of the GSK-3·ATP·pCREB (residues 119–146) model that included the C-terminal helix of pCREB as well, all soaked in water. The list of interactions in the final energy-minimized model is given in Table 1. In addition to the interactions between the

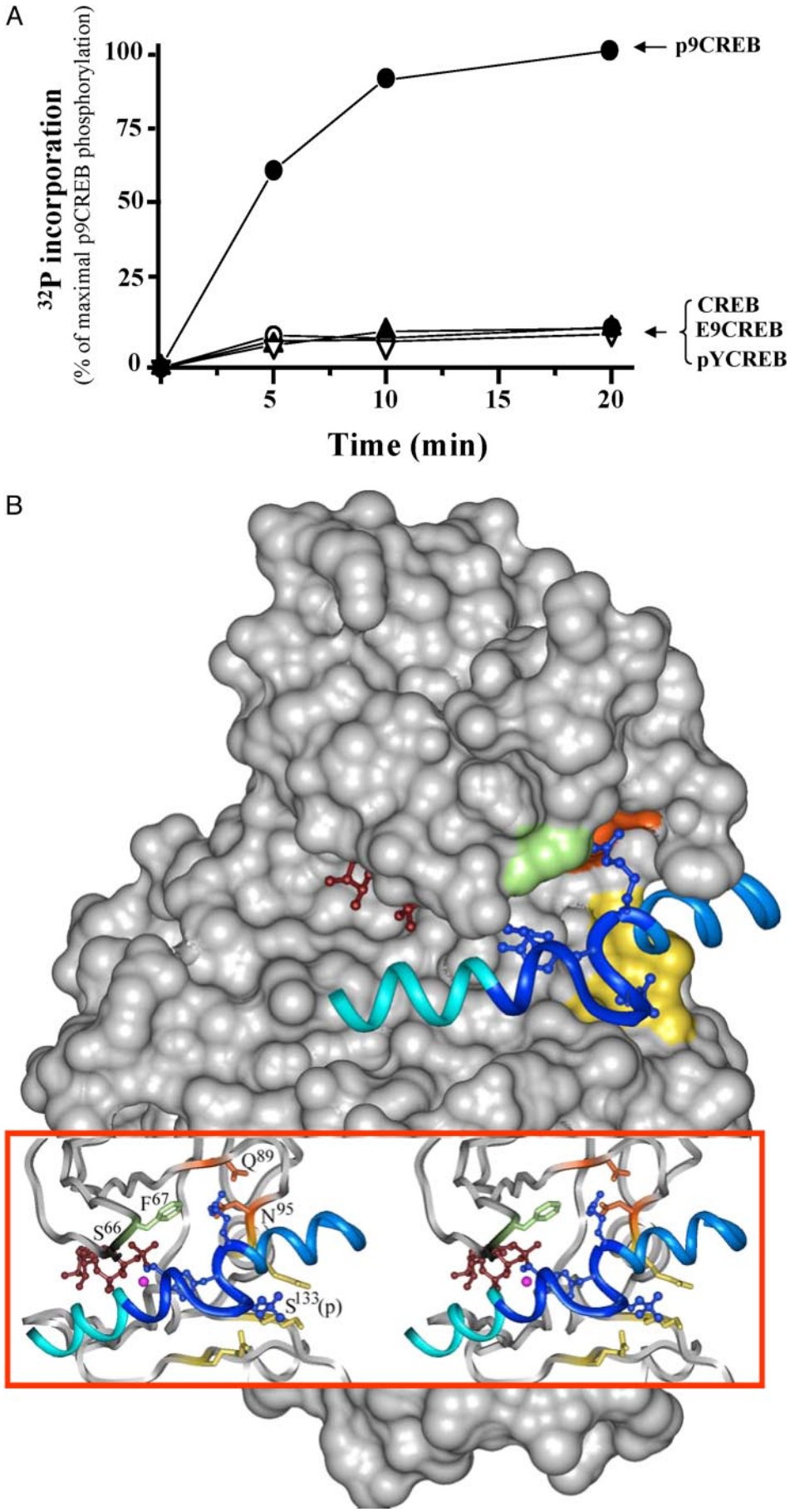

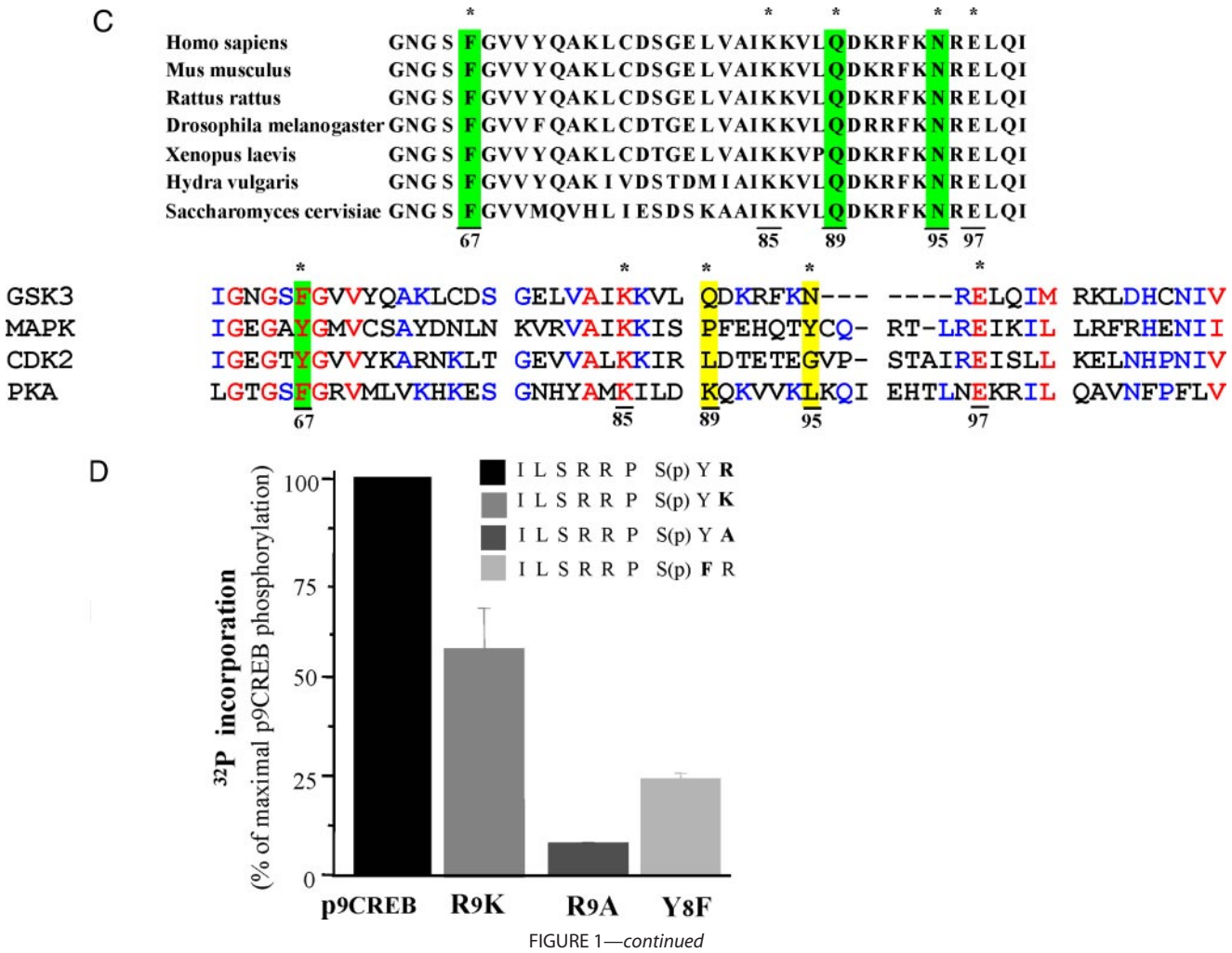

FIGURE 1—*continued*

phosphorylation site and the primed site of pCREB and GSK-3·ATP mentioned above, we found that CREB-Arg^{135} (within the p9CREB fragment) forms hydrogen bonds with Asn^{95} and Gln^{89} of GSK-3β and CREB-Tyr^{134} interacts with Phe^{67} of the kinase and also makes a hydrogen bond to the ATP γ-phosphate. The interactions of p9CREB or pCREB with GSK3β are shown in Fig. 1*B*.

The amino acids Gln^{89} and Asn^{95} are good candidates for substrate binding. They are conserved preferentially in GSK-3β, but not in other protein kinases, including GSK-3 paralogs (Fig. 1*C*). In addition, these amino acids are positioned away either from the conserved ATP binding pocket or the activation segment, and they are surface-exposed. The amino acid Phe^{67}, on the other hand, is more generally conserved and located in the conserved P-loop, which binds ATP, (41). Phe^{67} is not directly involved in ATP binding (according to Ref. 31), but it may be important for stabilizing the conformational change in the P-loop brought about by ATP binding. In addition, however, Phe^{67} is surface exposed and in our model it points toward

FIGURE 1. **Phosphorylation of p9CREB and model structure of the ternary complex GSK-3β·ATP·pCREB.** *A*, phosphorylation of p9CREB peptide variants by GSK-3. His-tagged purified GSK-3 was incubated with p9CREB peptide variants in the presence of [γ-^{32}P]ATP, as described under "Experimental Procedures" for indicated time points. The reactions were spotted on p81 papers and counted for radioactivity. Phosphorylation is presented as a percentage of maximal phosphorylation obtained with p9CREB substrate. Shown is a mean of two independent experiments. *Full circles* represent p9CREB. *Empty circle*, *filled triangle*, and *empty inverted triangle* represent CREB, ECREB, and pYCREB, respectively. *B*, solvent accessible surface of GSK-3β is shown in *gray*. Residues Gln^{89} and Asn^{95} are emphasized in *orange*, residue Phe^{67} is colored in *light green*, Ser^{66} is shown (only in the inset) in *black* and the positive primed phosphate binding site is depicted in *yellow*. The *ribbon diagram* in the insert (stereo pair) represents pCREB. The p9CREB fragment is colored in *dark blue* and the N- and C-terminal helices are colored in *cyan* and *blue*, respectively. The side chains of residues Ser^{129} (phosphorylation site), Ser^{133}(p) (primed phosphorylation site), Tyr^{134} and Arg^{135}, (which interact with Phe^{67} or Gln^{89} and Asn^{95}, respectively) are shown. ATP is shown as *brown ball* and *stick* model, and the Mg^{+2} ion is depicted by the *magenta sphere*. *C*, amino acid sequence alignment of the catalytic domain of GSK-3β in various species (as produced with the program ClustalW) and alignment of GSK-3β paralogs (CDK-2 and MAPK) and PKA. The latter sequence alignment is based on manual structural alignments (using the program InsightII) of the relevant structures (PDB codes, 1o9u, 1jst, 2erk, and 2cpk, respectively). The numbering corresponds to that of GSK-3. Potential residues for substrate recognition are denoted by *yellow* or *green* (identical residues) background. It shows that Gln^{89} and Asn^{95} are preferentially conserved in GSK-3. Conserved residues in all sequences are denoted by *red letters*; residues conserved in two or three sequences are denoted by *blue letters*. The residues mutated in this study are marked with an *asterisk*. *D*, ability of GSK-3 to phosphorylate p9CREB variants, was examined in assay conditions similar to those described in *A* (and under "Experimental Procedures"). Results are presented as the percentage of the phosphorylation obtained with p9CREB as a substrate that was set to 100%, and are mean of three independent experiments.

the substrate binding cavity, making it a potential hydrophobic contact with substrates.

In Vitro—To test the molecular modeling results, we replaced Arg^{9} in p9CREB (corresponding to Arg^{135}) by lysine or alanine, and Tyr^{8} (corresponding to Tyr^{134}) by phenylalanine. *In vitro* phosphorylation assays showed reduced ability of GSK-3β to phosphorylate R9K and Y8F. Replacement of R^{9} by alanine completely abolished phosphorylation (Fig. 1*D*). These results supported the model structure of GSK3·ATP·CREB described above, indicating that the hydrogen bonding interactions between Arg^{9} in p9CREB and GSK-3β are essential for substrate binding. Similarly, the hydrogen bonding interactions of Tyr^{8} have a role in substrate recognition.

Expression of GSK-3 Mutants in Escherichia coli and Their Autocatalytic Activity—To explore the role of residues Phe^{67}, Gln^{89}, and Asn^{95} in GSK-3-substrate recognition, we generated GSK-3β mutants and investigated their ability to phosphorylate substrates using *in vitro* and cellular systems. GSK-3 mutants in which residues Phe^{67}, Gln^{89}, or Asn^{95} were replaced by alanine were generated and expressed as His-tagged proteins (termed here Q89A, N95A, and F67A). Three additional mutants were used as controls. A kinase-dead mutant KK85,86MA in which ATP binding was prevented (6), termed here KI, E97A mutant in which the conserved glutamic acid located in the αC-helix participating in phosphoryl transfer (42) was replaced by alanine, and S66A mutant in which Ser^{66} was replaced by alanine. Ser^{66} is located near the enzyme-substrate binding site; however its hydrogen bond interaction with the substrate, as predicted by the model, is solvent-exposed and is not likely to contribute significantly to the binding (Fig. 1*B* and Table 1).

Expression of purified GSK-3β proteins was determined by Coomassie-stained gels or by immunoblot analysis using the GSK-3β antibody (Fig. 2, *A* and *B*). Both analyses confirmed that all proteins were expressed at similar levels. Phosphorylation of GSK-3β at Tyr^{216} reflects its autocatalytic activity (7). Thus, Tyr^{216} phosphorylation levels were determined by immunoblot analysis using the anti-phospho-GSK-3-Tyr^{216} antibody. Results show that, similar to wild-type, Q89A, N95A, F67A, and S66A mutants were tyrosine-phosphorylated. KI and E97A were not phosphorylated on Tyr^{216} (Fig. 2*A*). These results indicated that mutation at Gln^{89}, Asn^{95}, Phe^{67}, and Ser^{66} did not impair the intrinsic catalytic activity of the enzyme, whereas mutation at Glu^{97} resulted in an inactive mutant. The ability of F67A to autophosphorylate suggested that Phe^{67} is not critical for ATP binding as indeed previously indicated (31).

Phosphorylation of CREB Peptide by GSK-3 Mutant Proteins—The following experiments examined whether F67A, Q89A, and N95A mutant proteins can phosphorylate p9CREB. GSK-3β proteins were subjected to *in vitro* kinase assays using p9CREB as the substrate, and the amount of incorporated phosphorylation into the peptide was determined. As shown in Fig. 2*B*, Q89A displayed reduced phosphorylation ability toward p9CREB, as compared with WT GSK-3 (about 75% reduction),

TABLE 1

The interactions between GSK-3·ATP and pCREB as seen in our final model structure

The interactions of p9CREB are emphasized in bold font.

GSK3 residue	CREB residue	Type of interaction
Gln^{89}	**Arg^{135}**	**H-bond**
Asn^{95}	**Arg^{135}**	**H-bond**
ATP-γPO_3	**Tyr^{134}**	**H-bond**
Ser^{66}	Arg^{130}	Exposed H-bond
Arg^{96}	Asp^{140}	Exposed H-bond
Phe^{67}	**Tyr^{134}**	**Aromatic**
Phe^{93}	Leu^{138}	Hydrophobic
Val^{214}	Pro^{132}	Hydrophobic
Tyr^{216}(p)	**Ile^{127}**	**Hydrophobic**
Tyr^{216}(p)	Leu^{128}	Hydrophobic
Asp^{200}	Arg^{125}	Charged
Arg^{96}	**Ser^{133}(p)**	**Charged**
Arg^{180}	**Ser^{133}(p)**	**Charged**
Lys^{205}	**Ser^{133}(p)**	**Charged**
Tyr^{216}(p)	Arg^{124}	Charged
ATP-αPO_3	Arg^{126}	Charged

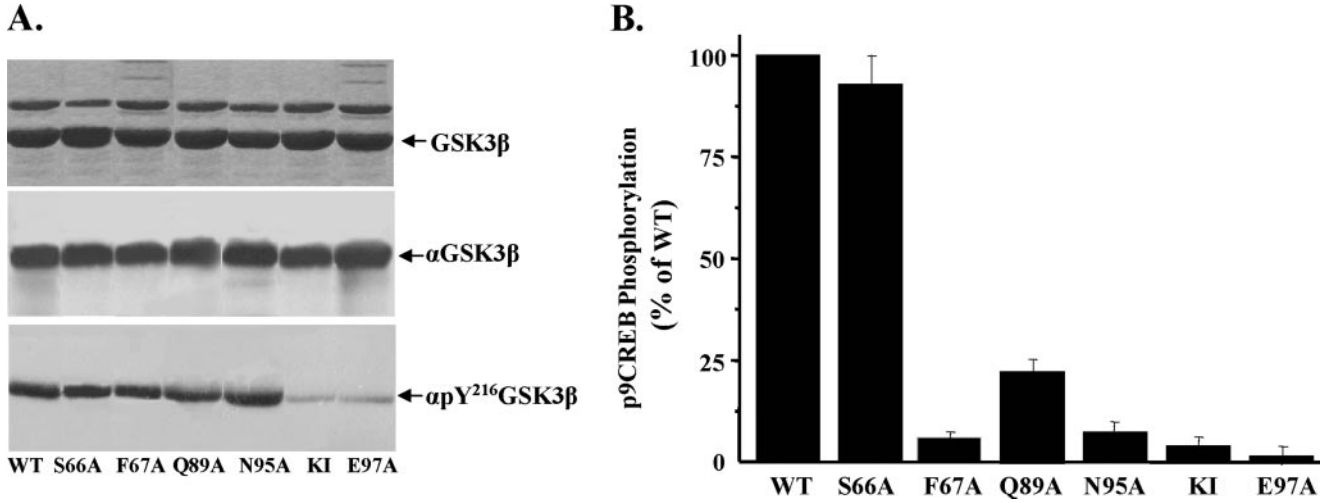

FIGURE 2. **Expression of GSK-3 mutants in *E. coli*.** *A*, His-tagged wild-type GSK-3 and GSK3 mutant proteins (F67A, S66A, Q89A, N95A, KK85, 86MA, E97A) were purified by affinity chromatography on Talon resin, as described under "Experimental Procedures." Total protein from each purification was subjected to gel electrophoresis and either stained with Coomassie Blue (*upper*), or subjected to immunoblot analysis with αGSK-3β antibody or αpY^{216}GSK-3 as indicated. *B*, phosphorylation of p9CREB with GSK-3 proteins was performed as described in the legend to Fig. 1*A* under "Experimental Procedures." The phosphorylation of p9CREB by mutant GSK3 proteins was expressed as a percentage of that obtained with wild-type which was set to 100%. The results are the mean of six independent experiments ± S.E. Results were statistically significant at $p < 0.01$.

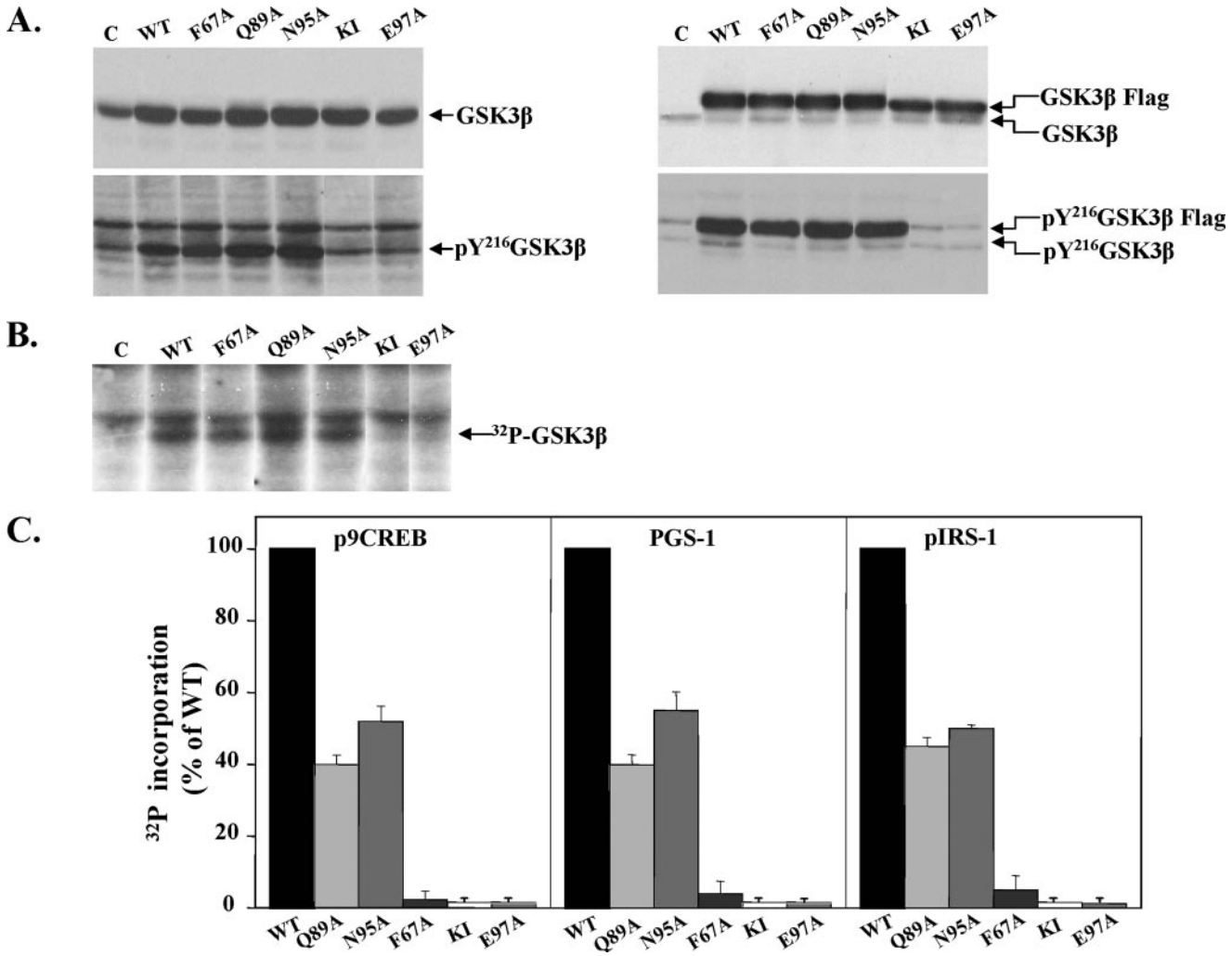

FIGURE 3. **Expression of GSK-3 mutants in cells.** *A*, cells were transiently transfected with DNA constructs expressing wild-type GSK-3, Q89A, N95A, F67A, KI, and E97A mutant proteins, as described under "Experimental Procedures." Cell extracts were subjected to Western blot analysis with either αGSK-3β antibody or αpTyr^{216}GSK-3 antibody, as indicated. Control (*C*) represents extracts from cells expressing the empty vector. *Left panel* shows results obtained with non-tagged GSK-3β, and *right panel* presents results obtained with FLAG-tagged GSK-3β. *B*, GSK-3β mutants were partially purified from expressing cells, as described under "Experimental Procedures," and were incubated for 20 min at 30 °C in the presence of [γ-^{32}P]ATP. Reactions were subjected to gel electrophoresis, and autoradiographed. Indicated is phosphorylated GSK-3β. *C*, phosphorylation of peptide substrates by GSK-3 mutant proteins. Equal amounts of partial purified GSK-3 proteins prepared as described under "Experimental Procedures" were subjected to *in vitro* kinase assays with p9CREB, PGS1, and pIRS-1 peptide substrates as described in the legend to Fig. 1*A* under "Experimental Procedures." ^{32}P incorporation into substrates was determined, and the activity obtained from control non-transfected cells was subtracted from each sample. Results present the percentage of substrate phosphorylation obtained with wild-type GSK-3 which was set to 100%, and are mean of five independent experiments each performed in duplicates. Expression levels of GSK-3 used in the assays are shown. Results were statistically significant ($p < 0.01$ mutant *versus* WT). For *A* and *B* shown representative gel of three independent experiments.

and N95A or F67A were unable to phosphorylate the peptide. The inactive mutants E97A and KI did not phosphorylate the peptide as expected. In addition, and as predicted, the negative control mutant S66A-phosphorylated p9CREB. These results supported the notion that Gln^{89}, Asn^{95}, and Phe^{67} (but not Ser^{66}) are important determinants for recognition of the p9CREB substrate by GSK-3β.

In Vivo Expression of GSK-3 Mutants in Cells and Phosphorylation of Substrates—It was important to demonstrate that the defected phosphorylation ability of GSK-3 mutants observed *in vitro* also occurs *in vivo*. For that, wild-type and Q89A, N95A, F67A, KI, and E97A cDNA expression vectors were transiently transfected in HEK-293 cells. FLAG-tagged or non-tagged GSK-3 constructs were used initially. All mutant proteins were expressed at similar levels and FLAG-tagged proteins were readily distinguished from endogenous GSK-3β (Fig. 3*A*). Immunoblot analysis of the same samples with the anti-phospho-Tyr^{216} antibody revealed that both tagged and non-tagged GSK-3 mutant proteins Q89A, N95A, and F67A were tyrosine-phosphorylated, whereas E97A and KI displayed (as expected) a very weak signal (Fig. 3*A*). These results indicated that mutations at Gln^{89}, Asn^{95}, and Phe^{67} did not abrogate the catalytic activity, because tyrosine phosphorylation of GSK-3 is mainly an intramolecular autophosphorylation process (6, 7). This conclusion is further supported by the observation that the inactive mutants were not tyrosine-phosphorylated (Fig. 3*A*).

Because overexpression of GSK-3 proteins was considerably above endogenous GSK-3 (Fig. 3), we chose to perform our experiments with the non-tagged GSK-3 constructs. The ability of GSK-3 mutants to autophosphorylate was examined in *in vitro* kinase assays. GSK-3 proteins were partially purified from cell extracts by ion exchange chromatography. The enzymes

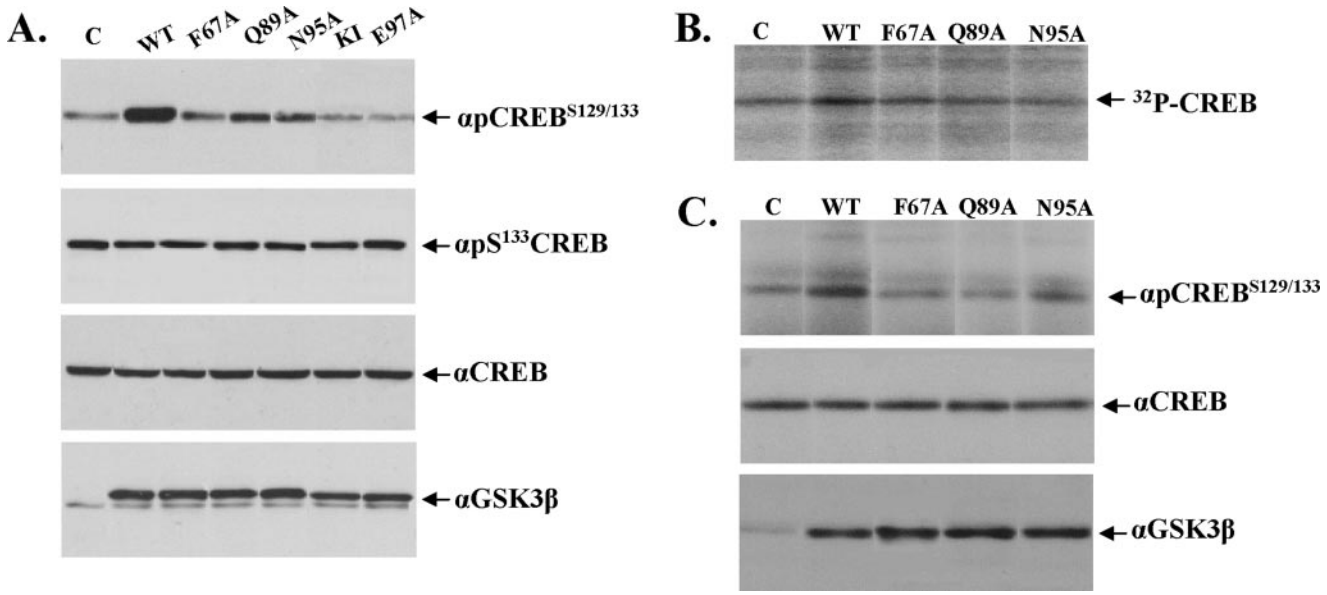

FIGURE 4. **Phosphorylation of cellular CREB by GSK-3 mutant proteins.** *A*, cells were co-expressed with GSK-3 and EGFP-CREB constructs. Cells were treated with forskolin for 30 min and lysed, as described under "Experimental Procedures." Equal amounts of protein aliquots were subjected to gel electrophoresis, followed by immunoblot analysis with αpCREB-Ser$^{129/133}$, αpCREB^{133}, or αCREB antibodies, as indicated. The expression levels of GSK-3 mutants in each sample are shown. Control (*C*) cells transfected with EGFP-CREB and pCMV4 empty vector. *B*, EGFP-CREB was overexpressed in cells. The protein was immunoprecipitated from cell extracts with anti-GFP antibody. GSK-3 mutant proteins were added to immunoprecipitates in the presence of [γ-^{32}P]ATP. Reactions were separated by gel electrophoresis and autoradiographed. Control (*C*) EGFP-CREB immunoprecipitate with no GSK-3. *C*, same as *B*, except that non-labeled ATP was used. Reactions were subjected to immunoblot analysis with αpCREB Ser$^{129/133}$. Expression levels of CREB or GSK-3 in each reaction is shown. For *A–C* shown a representative gel of three independent experiments.

were incubated with [γ-^{32}P]ATP, and phosphorylation was detected by gel electrophoresis (Fig. 3*B*). All three mutants were able to autophosphorylate supporting the view that their catalytic activity is not impaired. The ability of GSK-3 mutants to phosphorylate p9CREB substrate was tested next. As shown in Fig. 3*C*, Q89A and N95A displayed reduced phosphorylation toward p9CREB as compared with the wild-type, and F67A completely failed to phosphorylate the substrate. To further examine whether these findings are general, two additional substrates were used: PGS-1, a phosphorylated peptide derived from a GSK-3-substrate, glycogen synthase (24, 26), and pIRS-1, a phosphorylated peptide based on GSK-3-phosphorylation sequence in insulin receptor substrates-1 (IRS-1) (33). Similar results were obtained: Q89A and N95A displayed reduced phosphorylation toward PGS-1 and pIRS-1 substrates (about 50%), as compared with the wild-type, and F67A did not phosphorylate any of these substrates. These results suggested that Gln^{89} and Asn^{95} are indeed important determinants for substrate recognition by GSK-3. We noted that the phosphorylation ability of cellular-expressed N95A differs from the corresponding bacterially expressed mutant that was unable to phosphorylate p9CREB (Fig. 2*B*). We cannot provide a full explanation for this observation, although it is quite possible that post-translational modifications that do not occur in prokaryotes improved the ability of N95A to interact with the substrate. In any event, the results obtained from both expression systems (*i.e.* bacteria and mammalian cells) indicated that Gln^{89} and Asn^{95} play important roles in the substrate recognition mechanism. Phe^{67}, which is conserved among protein kinases, may also have a general role in kinase function, such as stabilization of the correct conformation for ATP binding. We cannot distinguish between these two roles, namely substrate binding (as predicted by the model) and conformational stabilization of the P-loop.

Phosphorylation of Cellular CREB by GSK-3 Mutant Proteins—The phosphorylation of cellular CREB by GSK-3 mutants was tested next. GSK-3 mutants were co-transfected with EGFP-CREB in HEK-293 cells. Notably, GSK-3 requires pre-phosphorylation of CREB at Ser^{133} (40). Therefore, cells were first treated with forskolin to activate PKA phosphorylation of CREB. The phosphorylation of CREB at the GSK-3 phosphorylation site Ser^{129} was determined by immunoblot analysis using a specific anti-phospho-CREB antibody that recognizes CREB phosphorylated at both Ser$^{129/133}$. Expression of wild-type GSK-3 increased phosphorylation of CREB Ser$^{129/133}$ significantly. However, expression of Q89A or N95A mutants resulted only in very weak CREB phosphorylation at these sites (Fig. 4*A*); expression of F67A did not increase CREB phosphorylation, which was comparable to that observed in "control" cells expressing EGFP-CREB alone. Notably, phosphorylation of CREB at Ser^{133}, as determined by a specific anti-phospho antibody, was unchanged in all samples, thus verifying that the changes observed with the "double" anti-phospho antibody reflected the changes in the GSK-3 phosphorylation site, Ser^{129}. Hence, mutations at Phe^{67}, Gln^{89}, and Asn^{95} impaired GSK-3 ability to phosphorylate cellular CREB.

To further investigate the above conclusion, we performed *in vitro* analyses with the "whole" protein CREB. In this experiment, EGFP-CREB was immunoprecipitated with anti-GFP antibody from overexpressing cells. The immunoprecipitate was incubated with GSK-3 wild-type and mutant proteins in hot or cold conditions. The hot reactions included [γ-^{32}P]ATP and were subjected to gel electrophoresis; ^{32}P incorporation into CREB protein was observed (Fig. 4*B*). The cold reactions

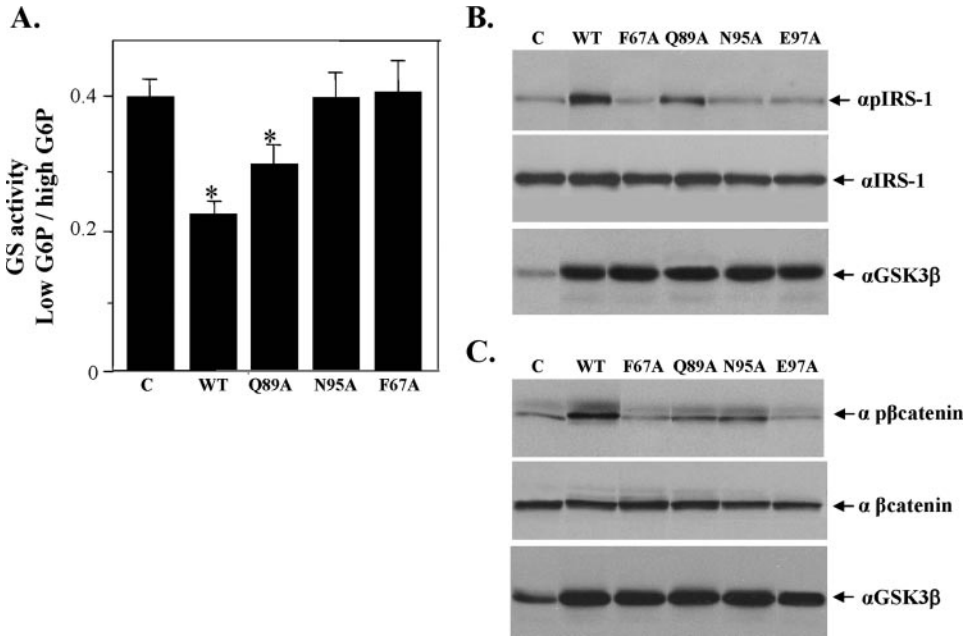

FIGURE 5. **The effect of GSK-3 mutants on glycogen Synthase, IRS-1, and β-catenin.** *A*, GS activity was measured in extracts prepared from cells expressing GSK-3 mutants. Results are expressed as activity ratio of reactions performed with low G6P or high G6P and are mean of three independent experiments ± S.E. Control (*C*) represents GS activity ratio measured in cells expressing pCMV4 empty vector only. *, $p < 0.01$ WT or mutant *versus* control. *B*, cells were transiently transfected with GSK-3 and IRS-1 constructs. Equal amounts of protein aliquots prepared from cells were subjected to gel electrophoresis, followed by immunoblot analysis with αpIRS-1 Ser^{332}, αIRS-1 antibody, or αGSK-3β. Control (*C*) cells expressing IRS-1, and the empty vector (pCMV4) *C*, cells were co-expressed with GSK-3 and GFP-β-catnein constructs, and cell extracts were prepared as described under "Experimental Procedures." Equal amounts of protein aliquots were subjected to gel electrophoresis, followed by immunoblot analysis with αp β-catenin antibody ($Ser^{33,37}$ and Thr^{41}) or α,β-catenin antibodies as indicated. The expression of GSK-3 mutants in each sample is shown. Control (*C*) cells expressing GFP-β-catenin and empty vector (pCMV4). For *B* and *C*, a representative gel of three independent experiments is shown.

were subjected to immunoblot analysis with the anti-phospho-$CREB^{129/133}$ antibody (Fig. 4*C*). Results showed that CREB protein was barely phosphorylated by Q89A, N95A, and F67A.

The Effect of GSK-3 Mutant Proteins on Glycogen Synthase Activity and Phosphorylation of IRS-1 and β-Catenin Substrates—The following experiments examined how GSK-3 mutants affect additional cellular substrates including glycogen synthase, insulin receptor substrate-1 (IRS-1), and β-catenin. Glycogen synthase (GS) is inhibited by GSK-3 via phosphorylation on a cluster of serine sites (43). We showed previously that overexpression of GSK-3 suppressed GS activity (6). Hence, it was possible to determine whether GSK-3 mutants suppress GS activity. We found that expression of wild-type GSK-3 suppressed GS activity by 50% ±10 (Fig. 5*A*), the mutant Q89A suppressed the enzyme by only 27% ± 8, and mutants N95A and F67A had no effect on GS activity (Fig. 5*A*). Thus F97A and N95A showed severely impaired ability toward suppression of GS activity.

In a different set of experiments, GSK-3 constructs were co-expressed with wild-type IRS-1 plasmid in HEK 293 cells. The GSK-3 phosphorylation site on IRS-1 is Ser^{332} and its phosphorylation can be detected by a specific antibody (33). IRS-1 phosphorylation increases significantly when co-expressed with GSK-3. Co-expression with Q89A increased IRS-1 phosphorylation to a much lesser extent and co-expression with N95A did not lead to detected increased phosphorylation of IRS-1 (Fig. 5*B*). These results are in line with the results obtained in the GS phosphorylation experiments, namely that Asn^{95} and Gln^{89} do not play equivalent roles in affecting IRS-1 or GS phosphorylation.

Collectively, it appears that Asn^{95} is more important than Gln^{89} for GS and IRS-1 recognition. Interestingly, both GS and IRS-1 have aspartic acid residues in the position corresponding to Arg^{9} of p9CREB (position +2 from the primed site). Possibly the shorter side chain of aspartic acid, compared with arginine, interacts with Asn^{95} and less with Gln^{89}. The difference between the results obtained for substrate peptides and substrate proteins can be attributed to the greater flexibility of peptides as compared with the corresponding fragments within proteins, which enables the peptides to adjust and form better contacts with the GSK-3 mutants than the corresponding proteins.

β-Catenin is a key downstream target in *Wnt* signaling pathway and a substrate of GSK-3 phosphorylated at $Ser^{33,37}$ and Thr^{41} (44). Phosphorylation of Ser^{45} in β-catenin by casein kinase-1 (CKI), serves as a priming site for subsequent phosphorylation by GSK3 (44, 45). GSK-3 constructs were co-expressed together with GFP-β-catenin plasmid in HEK-293 cells. Phosphorylation of β-catenin at GSK-3β phosphorylation sites was detected with specific anti-phospho β-catenin antibody as shown in Fig. 5*C*. Q89A and N95A were able to phosphorylate β-catenin *albeit* to a significantly lower extent as compared with wide-type GSK-3. Consistently, F67A was unable to phosphorylate β-catenin. Notably, position +2 in β-catenin is occupied by a small polar side chain (serine), which is likely to make fewer interactions with GSK-3.

The similar results obtained for the various GSK-3 substrates suggested that a common mechanism controls substrates recognition. This mechanism involves interactions with Gln^{89} and Asn^{95} and possibly Phe^{67} in addition to the interactions with the primed phosphate binding pocket. The ability to interact with diverse substrate motives is explained by the polar nature of Gln^{89} and Asn^{95}, which enables them to form hydrogen bonds with various polar/charged residues. As discussed above, the exact role of Phe^{67} is not clear.

In conclusion, our studies gained important additional understanding of how GSK-3β recognizes its substrates. On one level, GSK-3β binds a phosphorylated substrate by a well-defined, positively charged pocket (27, 28, 46), which filters away non-phosphorylated substrates. On the second level, additional interactions are necessary to facilitate precise positioning of the substrate within the substrate binding pocket, with the target serine located next to the ATP γ-phosphate.

This is achieved by interaction with Gln^{89}, Asn^{95}, and possibly Phe^{67}. We highlight the roles of Gln^{89} and Asn^{95}, which are preferentially conserved in GSK-3β, and are polar residues that can participate in hydrogen bonding with various polar/charged residues, allowing both tight binding and the ability to interact with a broad selection of substrates. Recognition, thus, combines the highly specific primed phosphorylation recognition, and moderately specific hydrogen bond interactions that together determine the substrate specificity toward the kinase.

REFERENCES

1. Woodgett, J. R. (1990) *EMBO J.* **9,** 2431–2438
2. Bardwell, A. J., Flatauer, L. J., Matsukuma, K., Thorner, J., and Bardwell, L. (2001) *J. Biol. Chem.* **276,** 10374–10386
3. Doble, B. W., and Woodgett, J. R. (2003) *J. Cell Sci.* **116,** 1175–1186
4. Grimes, C. A., and Jope, R. S. (2001) *Prog. Neurobiol.* **65,** 391–426
5. Hughes, K., Nicolakaki, E., Plyte, S. E., Totty, N. F., and Woodgett, J. R. (1993) *EMBO J.* **12,** 803–808
6. Eldar-Finkelman, H., Agrast, G. M., Foord, O., Fischer, E. H., and Krebs, E. G. (1996) *Proc. Natl. Acad. Sci. U. S. A.* **93,** 10228–10233
7. Cole, A., Frame, S., and Cohen, P. (2004) *Biochem. J.* **377,** 249–255
8. Eldar-Finkelman, H. (2002) *Trend. Mol. Med.* **8,** 126–132
9. Woodgett, J. R. (2003) *Curr. Drug Targets Immune. Endocr. Metabol. Disord.* **3,** 281–290
10. Gould, T. D., Zarate, C. A., and Manji, H. K. (2004) *J. Clin. Psychiatry* **65,** 10–21
11. Coghlan, M. P., Culbert, A. A., Cross, D. A., Corcoran, S. L., Yates, J. W., Pearce, N. J., Rausch, O. L., Murphy, G. J., Carter, P. S., Roxbee Cox, L., Mills, D., Brown, M. J., Haigh, D., Ward, R. W., Smith, D. G., Murray, K. J., Reith, A. D., and Holder, J. C. (2000) *Chem. Biol.* **7,** 793–803
12. Cline, G. W., Johnson, K., Regittnig, W., Perret, P., Tozzo, E., Xiano, L., Damico, C., and Shulman, G. I. (2002) *Diabetes* 2903–2910
13. Plotkin, B., Kaidanovich, O., Talior, I., and Eldar-Finkelman, H. (2003) *J. Pharmacol. Exp. Ther.* 974–980
14. Martinez, A., Alonso, M., Castro, A., Perez, C., and Moreno, F. J. (2002) *J. Med. Chem.* **45,** 1292–1299
15. Kemp, B. E., and Pearson, R. B. (1990) *Trends Biochem. Sci.* **15,** 342–346
16. Yaffe, M. B., Rittinger, K., Volinia, S., Caron, P. R., Aitken, A., Leffers, H., Gamblin, S. J., Smerdon, S. J., and Cantley, L. C. (1997) *Cell* **91,** 961–971
17. Brinkworth, R. I., Breinl, R. A., and Kobe, B. (2003) *Proc. Natl. Acad. Sci. U. S. A.* **100,** 74–79
18. Yaffe, M. B. (2004) *Methods Mol. Biol.* **250,** 237–250
19. Alto, N. M., Soderling, S. H., Hoshi, N., Langeberg, L. K., Fayos, R., Jennings, P. A., and Scott, J. D. (2003) *Proc. Natl. Acad. Sci. U. S. A.* **100,** 4445–4450
20. Taylor, S. S., Radzio-Andzelm, E., and Hunter, T. (1995) *FASEB J.* **9,** 1255–1266
21. Padilla, A., Hauer, J. A., Tsigelny, I., Parello, J., and Taylor, S. S. (1997) *J. Pept. Res.* **49,** 210–220
22. Narayana, N., Cox, S., Shaltiel, S., Taylor, S. S., and Xuong, N. (1997) *Biochemistry* **36,** 4438–4448
23. Yang, J., Cron, P., Good, V. M., Thompson, V., Hemmings, B. A., and Barford, D. (2002) *Nat. Struct. Biol.* **9,** 940–944
24. Woodgett, J. R., and Cohen, P. (1984) *Biochim. Biophys. Acta* **788,** 339–347
25. Fiol, C. J., Mahrenholz, A. M., Wang, Y., Roeske, R. W., and Roach, P. J. (1987) *J. Biol. Chem.* **262,** 14042–14048
26. Roach, P. J. (1991) *J. Biol. Chem.* **266,** 14139–14142
27. ter Haar, E., Coll, J. T., Austen, D. A., Hsiao, H. M., Swenson, L., and Jain, J. (2001) *Nat. Struct. Biol.* **8,** 593–596
28. Dajani, R., Fraser, E., Roe, S. M., Young, N., Good, V., Dale, T. C., and Pearl, L. H. (2001) *Cell* **105,** 721–732
29. Bax, B., Carter, P. S., Lewis, C., Guy, A. R., Bridges, A., Tanner, R., Pettman, G., Mannix, C., Culbert, A. A., Brown, M. J., Smith, D. G., and Reith, A. D. (2001) *Structure* **9,** 1143–1152
30. Dajani, R., Fraser, E., Roe, S. M., Yeo, M., Good, V. M., Thompson, V., Dale, T. C., and Pearl, L. H. (2003) *EMBO J.* **22,** 494–501
31. Bertrand, J. A., Thieffine, S., Vulpetti, A., Cristiani, C., Valsasina, B., Knapp, S., Kalisz, H. M., and Flocco, M. (2003) *J. Mol. Biol.* **333,** 393–407
32. Radhakrishnan, I., Perez-Alvarado, G. C., Parker, D., Dyson, H. J., Montminy, M. R., and Wright, P. E. (1997) *Cell* **91,** 741–752
33. Liberman, Z., and Eldar-Finkelman, H. (2005) *J. Biol. Chem.* **280,** 4422–4428
34. Berman, H. M., Westbrook, J., Feng, Z., Gilliland, G., Bhat, T. N., Weissig, H., Shindyalov, I. N., and Bourne, P. E. (2000) *Nucleic Acids Res.* **28,** 235–242
35. Katchalski-Katzir, E., Shariv, I., Eisenstein, M., Friesem, A. A., Aflalo, C., and Vakser, I. A. (1992) *Proc. Natl. Acad. Sci. U. S. A.* **89,** 2195–2199
36. Ben-Zeev, E., and Eisenstein, M. (2003) *Proteins* **52,** 24–27
37. Heifetz, A., Katchalski-Katzir, E., and Eisenstein, M. (2002) *Protein Sci.* **11,** 571–587
38. Berchanski, A., Shapira, B., and Eisenstein, M. (2004) *Proteins* **351,** 309–326
39. Thomas, J. A., Schlender, K. K., and Larner, J. (1968) *Anal. Biochem.* **25,** 486–499
40. Fiol, C. J., Williams, J. S., Chou, C. H., Wang, Q. M., Roach, P. J., and Andrisani, O. M. (1994) *J. Biol. Chem.* **269,** 32187–32193
41. Saraste, M., Sibbald, P. R., and Wittinghofer, A. (1990) *Trends Biochem. Sci.* **15,** 430–434
42. Bhat, R., Xue, Y., Berg, S., Hellberg, S., Ormo, M., Nilsson, Y., Radesater, A. C., Jerning, E., Markgren, P. O., Borgegard, T., Nylof, M., Gimenez-Cassina, A., Hernandez, F., Lucas, J. J., Diaz-Nido, J., and Avila, J. (2003) *J. Biol. Chem.* **278,** 45937–45945
43. Woodgett, J. R., and Cohen, P. (1984) *Biochim. Biophys. Acta* **788,** 339–347
44. Liu, C., Li, Y., Semenov, M., Han, C., Baeg, G. H., Tan, Y., Zhang, Z., Lin, X., and He, X. (2002) *Cell* **108,** 837–847
45. Yanagawa, S., Matsuda, Y., Lee, J. S., Matsubayashi, H., Sese, S., Kadowaki, T., and Ishimoto, A. (2002) *EMBO J.* **21,** 1733–1742
46. Frame, S., and Cohen, P. (2001) *Biochem. J.* **359,** 1–16